Dynamic Heterogeneity in Fully Miscible Blends of Polystyrene with Oligostyrene

Vagelis A. Harmandaris,[3,†] Kurt Kremer,[2] and George Floudas[1,2,*]

[1]Department of Physics, University of Ioannina, GR-45110, Ioannina, Greece
[2]Max Planck Institute for Polymer Research, D-55128 Mainz, Germany
[3]Department of Applied Mathematics, University of Crete, and IACM FORTH GR-71110 Heraklion, Greece

(Received 29 October 2012; published 18 April 2013)

Binary blends of polystyrene with oligostyrene are perfectly miscible ($\chi = 0$) yet dynamically heterogeneous. This is evidenced by independent probing of the dipole relaxation perpendicular to the backbone by dielectric spectroscopy and molecular dynamics. The self-concentration model with a single intramolecular length scale qualitatively describes the slower segmental dynamics. A quantitative comparison based on MD, however, requires a composition-dependent length scale. The pertinent dynamic length scale that best describes the slow segmental dynamics in miscible blends relates to both intra- and intermolecular contributions.

DOI: 10.1103/PhysRevLett.110.165701 PACS numbers: 64.70.pj, 64.70.Q−, 77.22.Gm

Thermodynamically miscible polymer blends display a broadening of the relaxation spectra with respect to homopolymers and two separate relaxation processes that reflect the component's segmental dynamics. Both are considered as signatures of dynamic heterogeneities [1–6]. Theoretical models [7–17] have been considered in explaining these experimental features. In all cases, increasing the dynamic asymmetry, i.e., by increasing the difference in the glass temperatures (ΔT_g) of the parent homopolymers, enhances the dynamic heterogeneity. However, polymer mixtures with large disparity in their mobility are usually composed from monomers of different polarity and/or rigidity that tend to phase separately. In addition, even the known miscible blends show a miscibility window only for certain molecular weights, compositions, temperatures, and pressures. In the quest for the *truly* miscible blend with a large dynamic asymmetry an obvious choice is mixtures of a homopolymer with its oligomers.

Dielectric spectroscopy (DS) [4,6,8,11,12,14,15,18–24] and molecular dynamics (MD) simulations [16,17,25–32] represent versatile and complementary tools in studying segmental dynamics in polymer blends. In this Letter we report on the local dynamics in perfectly miscible blends of polystyrene with oligostyrene possessing a large dynamic asymmetry ($\Delta T_g = 123$ K) by MD and DS spanning about 12 decades in time. The blends display clear signatures of a dynamic heterogeneity as evidenced by the bimodal relaxation in both MD and DS. This allowed (i) testing the validity of the self-concentration model [9] and (ii) an independent and quantitative account for the slower dynamics through MD. The relation of the corresponding dynamic length scale with the static length scale corresponding to the static structure factor for the polymer chains is explored.

The studied homopolymer PS_{68} had $M_w = 7150$ g/mol and $M_n = 6800$ g/mol (about 65 monomers). The oligomer PS_3 had $M_w = M_n = 370$ g/mol. The tacticity of PS_{68} was obtained from ^{13}C NMR, giving 18% iso, 46% atactic, and 36% syndiotactic sequences. The blend dynamics was investigated by probing the dipole perpendicular to the backbone by DS and MD. The dielectric loss curves in the blend, shown in Fig. 1, are clearly bimodal with "slow" and "fast" processes reflecting the PS_{68} and PS_3 relaxations in the blends. Two Havriliak-Negami functions together with the conductivity contributions at lower frequencies or high temperatures are necessary to deconvolute the spectra (see the Supplemental Material [33] for the analysis of the DS and MD dynamics). Details about the all atom MD simulations employed in this study and the equilibration procedure are given elsewhere [30].

In MD simulations, the segmental dynamics of polymer melts can be studied by calculating time-autocorrelation functions of a vector, $\mathbf{v}_b$, along the monomer. Here we choose a vector that connects the carbon of the backbone CH group with the center of mass (CM) of the phenyl ring [30]. In more detail, segmental dynamics is quantified, in both MD and DS, through the first Legendre polynomial, $P_1(t) = \langle \cos[\theta(t)] \rangle$, where θ is the angle of $\mathbf{v}_b$ vector at time t relative to its original position.

Figure 2 depicts the $P_1(t)$ autocorrelation curves of the C-CM ring for the blends and the respective homopolymers at 463 K obtained from MD. $P_1(t)$ exhibits a small rapid decay at short times ($t < 10$–100 ps) followed by a rather slow decorrelation at later times. This short-time regime (not shown here) corresponds to a primitive (bond vibrations and angle librations) relaxation (Debye-Waller factor), whereas the long-time regime corresponds to the segmental relaxation. In agreement with DS, bimodality is evident in MD simulations as well. The $P_1(t)$ data were fitted (for times $t > 10$ ps) by a Kohlrausch-Williams-Watts (KWW) stretched-exponential function $P(t) = A \exp[-(t/\tau_{\mathrm{KWW}})^{\beta}]$ where, τ_{KWW}, is a characteristic relaxation time, β the stretch exponent, and A a

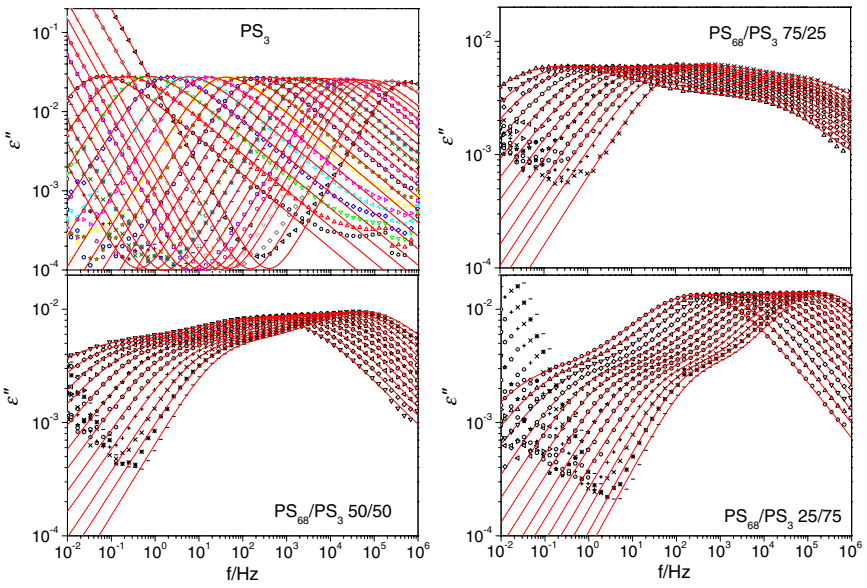

FIG. 1 (color online). Dielectric loss plotted as a function of frequency for the PS_3 oligomer (upper left, temperatures in the range from 237.15 to 283.15 K), the 75/25 blend (upper right, temperatures in the range from 319.15 to 336.15 K), the 50/50 blend (lower left, temperatures in the range from 281.15 to 303.15 K), and the 25/75 blend (lower right, temperatures in the range from 265.15 to 291.15 K). Lines are the result of fits to a summation of two Havriliak-Negami functions.

preexponential factor that takes into account relaxation processes at very short time scales. The segmental correlation time τ_s, defined as the integral of the above equation, can be calculated numerically and is presented below in Fig. 3. Fits of the simulation data for times above about 5–10 ps are included in Fig. 2 with lines. Note that a modified KWW expression, that describes fast relaxation modes with an additional exponential term, gives very similar values for both τ_{KWW} and β; see Supplemental Material [33]. The comparison of the stretch exponent, obtained independently from MD [Eq. (1)] and DS (Supplemental Material [33]) suggests the broadening of the slow component in the blend. This is explained by the increasing concentration fluctuations [8] on approaching the glass temperature of the slower component. Understanding the complete T dependence of the distribution requires knowledge of the separate contribution from temporal and spatial heterogeneities [34].

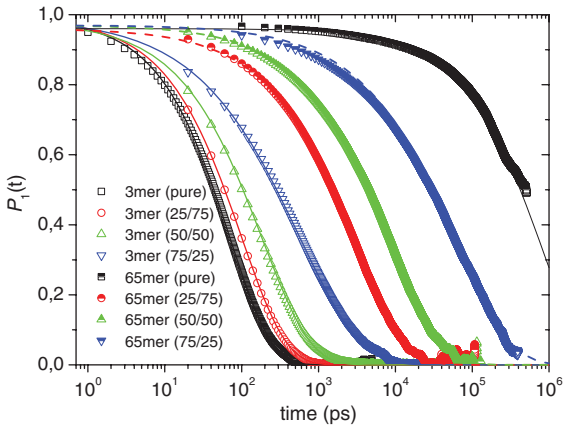

FIG. 2 (color). Time correlation function $P_1(t)$ for the PS 3mer and PS 65mer (PS_{68}) studied here from MD. The lines are KWW fits ($T = 463$ K).

The segmental dynamics from MD and DS comprising 13 orders of magnitude (for the 3mer) are directly compared in Fig. 3. The $\tau(T)$ conform to the Vogel-Fulcher-Tammann equation, $\tau = \tau_0 \exp[B/(T - T_0)]$, with parameters summarized in Table I of the Supplemental Material [33] (these lines are not shown in Fig. 3 for clarity).

According to the "self-concentration" model of Lodge and McLeish (LM) [9], the average composition of the local environment around any chosen segment is enriched by the same species because of chain connectivity effects. Each species will experience a different average local environment and to the extent that the glass temperature is sensitive to composition, each polymer will sense its own composition-dependent glass temperature. The relevant length scale in evaluating the self-concentration is the Kuhn length (l_K). The self-concentration of component i is determined from the volume fraction occupied by monomers in one Kuhn length inside a volume $V_K = {l_K}^3$ as $\varphi_{\mathrm{self},i} = C_\infty M_o / k \rho N_A V_k$ where C_∞ is the characteristic ratio, M_o is the repeat unit molar mass, and k is the number of backbone bonds per repeat unit of the component i, and N_A is the Avogadro number. The model associates the average local concentration of each component with a local glass temperature, $T_{g,\mathrm{eff}} = T_g(\varphi)|_{\varphi=\varphi_{\mathrm{eff}}}$. The effective glass temperature $T_{g,\mathrm{eff}}$ is determined from the macroscopic $T_g(\varphi)$ but now evaluated at φ_{eff}, which for two components A and B is defined as

$$\begin{aligned} \varphi_{\mathrm{eff},A} &= \varphi_{\mathrm{self},A} + (1 - \varphi_{\mathrm{self},A})\varphi_A, \\ \varphi_{\mathrm{eff},B} &= \varphi_{\mathrm{self},B} + (1 - \varphi_{\mathrm{self},B})\varphi_B, \end{aligned} \tag{1}$$

where φ_A and φ_A are the bulk volume fractions of A and B, respectively. Lipson and Milner [32] proposed a modification of the above expression that resulted in a self-consistent definition (i.e., self-consistent Lipson Milner, SCLM):

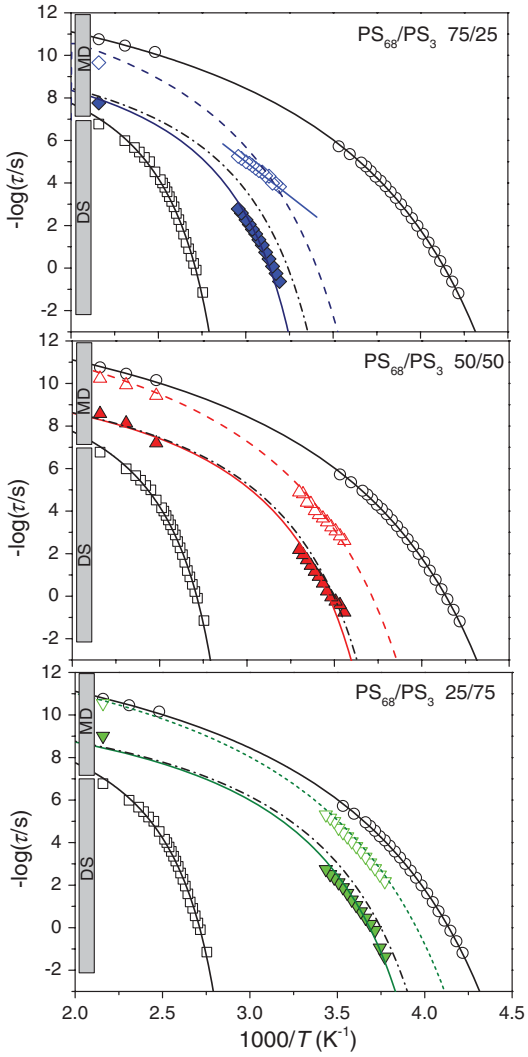

FIG. 3 (color). Arrhenius relaxation map of the segmental dynamics in the homopolymer PS_{68} (open squares) and PS_3 (open circles) and the PS_{68}/PS_3 blends (triangles) with composition: 75/25/ (top), 50/50 (middle), and 25/75 (bottom) obtained from MD (higher frequencies) and DS (lower frequencies). The slow and fast segmental dynamics in the blends are shown with filled and open symbols, respectively. In the blends the solid and dashed lines are fits based solely on MD predictions for self- and effective compositions Eq. (4) of the slow and fast dynamics using $\varphi_{\mathrm{self},A} = 0.48$ and $\varphi_{\mathrm{self},B} = 0.74$. The dash-dotted black line is the comparison to the SCLM model Eq. (2) with $\varphi_{\mathrm{self},A} = 0.26$. Notice the Arrhenius T dependence for the fast segmental dynamics in the 75/25 blend (confinement effects).

$$\varphi_{\mathrm{eff},A} = \varphi_{\mathrm{self},A} + (1 - \varphi_{\mathrm{self},A})p,$$
$$\varphi_{\mathrm{eff},B} = \varphi_{\mathrm{self},B} + (1 - \varphi_{\mathrm{self},B})(1 - p). \quad (2)$$

In the above relation, p, the probability that an intermolecular neighbor within a volume V_K is of type A regardless of the type of the central atom is given by

$$p = \frac{\varphi_A(1 - \varphi_{\mathrm{self},A})}{\varphi_A(1 - \varphi_{\mathrm{self},A}) + \varphi_B(1 - \varphi_{\mathrm{self},B})}. \quad (3)$$

For the macroscopic composition dependence of the glass temperature the model suggests the Fox equation [23]. However, the Fox equation cannot describe the "effective" T_g values in blends, the latter measured by DSC. Here we employed the Gordon-Taylor equation instead (with the value of the adjustable parameter $K = 3.08$).

In Fig. 3 we test the SCLM model predictions for the slow and fast component dynamics against the full $\tau(T)$ dependence. The three Arrhenius relaxation maps display the relaxation times of the PS_{68}, PS_3 homopolymers and three PS_{68}/PS_3 blends together with the SCLM model predictions [Eq. (2)] for the slower component (dash-dotted lines). φ_{self} for component A (PS_{68}) was calculated through the model using $C_\infty = 9.61$, $M_0 = 0.104$ kg/mol, $k = 2$, $\rho = 986$ kg/m^3, $l_K = 1.48$ nm resulting in $\varphi_{\mathrm{self},A} = 0.26$. It can be seen that the SCLM model predictions are in qualitative agreement with the slow PS_{68} segmental dynamics in the blends but not in quantitative agreement. Evidently, a single length scale cannot describe the full $\tau(T)$ dependence for all blend compositions. As for the relevant length scale for the oligomer (PS_3), we can employ the end-to-end distance of $l = 0.65$ nm ($r = 0.4$ nm; see below for the definition) from simulations. However, Eq. (3) gives an unphysical value of $\varphi_{\mathrm{self},B}$ (> 1) for such a length scale. For both segmental dynamics in the blends we have further assumed the Vogel-Fulcher-Tammann equation for $\tau_i(\varphi_{\mathrm{eff}}, T)$, with identical B_i and $\tau_{0,i}$ parameters as for bulk PS_{68} and PS_3 ($B = 1140$ K and $\tau_0 = 3.02 \times 10^{-11}$ s for PS_{68} and $B = 1680$ K and $\tau_0 = 3.63 \times 10^{-14}$ s for PS_3) where only the "ideal" glass temperature, $T_{0,i}(\varphi_{\mathrm{eff}}) = T_{0,i} + [T_{g,i}(\varphi_{\mathrm{eff}}) - T_{g,i}]$, varies with composition. $T_{0,i}$ is the ideal glass temperature for homopolymers A or B and $T_{0,i}(\varphi_{\mathrm{eff}})$ is the ideal glass temperature for each component in the blends. In addition, one can notice a peculiar T dependence (nearly Arrhenius) of the fast relaxation times in the more asymmetric PS_{68}/PS_3 75/25 blend [Fig. 3(a)]. This has been discussed in the literature as reflecting the dynamics of the faster component that is now confined within the frozen domains of the slower component [35]. Cleary, the model does not take into account such confinement effects that can lead to a Arrhenius temperature dependence.

In view of these deficiencies associated with the SCLM model, we employ MD simulations as a guide in predicting the effective composition for each component in the blends that best fit the combined DS/MD $\tau(T)$ dependence. In more detail, from the MD simulations we directly calculate apparent distance dependent self- and effective concentrations defined as

$$\varphi_{\mathrm{self},i}(r) = \frac{\langle M_i^{\mathrm{intra}}(r)\rangle}{\langle M_A(r) + M_B(r)\rangle},$$
$$\varphi_{\mathrm{eff},i}(r) = \frac{\langle M_i(r)\rangle}{\langle M_A(r) + M_B(r)\rangle}, \quad (4)$$

where $M_i(r)$ and $M_i^{\text{intra}}(r)$ are the total and the intramolecular atom mass of neighbors of type i (A or B) within a sphere with radius r around a central atom of type i. Brackets denote statistical average. Furthermore, we can also calculate effective concentrations by employing Eq. (1) (LM model) and Eq. (2) (SCLM model) using the values for $\varphi_{\text{self},i}$ and p calculated directly from the MD simulations.

In Figs. 4(a)–4(d) we present the MD result for self- and effective composition denoted as $\varphi_{\text{eff},i}$ MD, LM. and SCLM, calculated, respectively using Eqs. (4) and (1), or (2). Self-concentration, as expected, is much larger for 65mer than for 3mer for a given length scale and does not depend on the concentration. Notice that $\varphi_{\text{eff},i}$ obtained through MD differs substantially from the LM model. This is in agreement with earlier MD simulations that emphasized the importance of distributions of intramolecular concentrations on the dynamics especially in dilute blends [17]. A direct comparison of the simulation with the LM model can be made by calculating the composition within a sphere with the same volume as an $l_K{}^3$ cube, i.e., within a radius of $r = l_K/2 * (6/\pi)^{1/3} = 0.9$ nm, resulting in $\varphi_{\text{self},A} \sim 0.48$ [Fig. 4(a)]. For the oligomer (PS_3), we can employ the MD predictions at the relevant length scale ($r = 0.4$ nm) resulting in $\varphi_{\text{self},B} = 0.74$ [Fig. 4(a)].

According to MD, a quantitative description of the full $\tau(T)$ for the slower component, as shown in Fig. 3 with the color solid lines, requires $\varphi_{\text{eff},A} = 0.82$, 0.64, and 0.48, respectively, for the 75/25, 50/50, and 25/75 blends. The extracted (Fig. 4) dynamic length scale is plotted in Fig. 5 as a function of blend composition. Evidently, the dynamic length scale *decreases* with *increasing* polymer concentration (PS_{68}). In the same figure we plot (i) the purely intramolecular length scale from the LM model (l_K) and (ii) the concentration dependence of the pair atom-atom correlations in the intermolecular pair distribution function, $g(r)$, representing solely polymer correlations (PS_{68}). The latter shows a $d \sim \varphi^{-0.6}$ dependence that corresponds to the good solvent scaling for the blob size in concentrated solutions in a crossover regime to the melt ($\xi \sim \varphi^{\nu/1-3\nu}$ with $\nu_{\text{eff}} \sim 4/5$). The dynamic length scale, has a composition dependence ($\varphi^{-0.26}$), intermediate to the purely intermolecular ($\varphi^{-0.6}$) and intramolecular (φ^0) length scales. This suggests that both interactions should be taken into account in understanding the dynamics of the slow segmental dynamics in miscible blends.

Despite the success in understanding the slow segmental dynamics in the blends, the same cannot be said about the oligomer dynamics. The extracted length scales that best describe the $\tau(T)$ of the fast component (dashed lines in Fig. 3) exceeds the oligomeric end-to-end distance (lengths of 1.2, 0.9, and 2.2 nm are obtained for the 75/25, 50/50, and 25/75 blends).

In conclusion, binary blends of polystyrene with oligostyrene display dynamic heterogeneity at the segment level as evidenced by independent probing of the dipolar relaxation by dielectric spectroscopy and MD simulations. The self-concentration model with a single intramolecular length scale describes the segmental dynamics of the slow component in the blend with a $\varphi_{\text{self},A} \sim 0.26$, however, only qualitatively. A quantitative description requires a composition-dependent length scale. MD simulations of the effective composition coupled with the $\tau(T)$ dependence provide the relevant dynamic length scale. The latter exhibits a distinct concentration dependence, which is weaker as that of atom-to-atom correlations in the

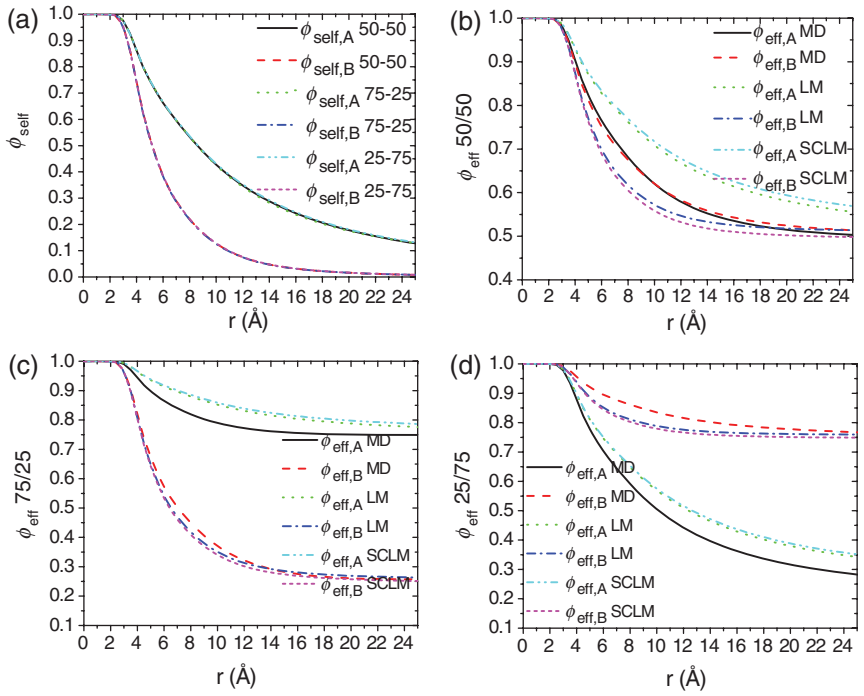

FIG. 4 (color). (a) Self-concentration for all binary blends and (b)–(d) effective concentrations for the different blends within a sphere as a function of the sphere radius calculated through MD simulations Eq. (4), LM Eq. (1), and SCLM model for $p = 0.51$ Eqs. (2) and (3) (for length scale radius of 0.9 nm and 0.4 nm for A and B, respectively; A is the 65mer and B the 3mer) at $T = 463$ K.

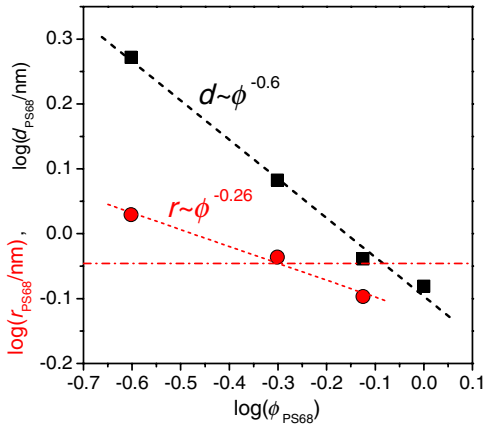

FIG. 5 (color online). Composition dependence of (i) the PS_{68} static correlations (d) corresponding to the intermolecular atom-to-atom correlations in the blends (squares), and (ii) of the sphere radius (circles) that provides the best description of the slower segmental dynamics in the blends (r). The corresponding Kuhn length scale (l_K) is also shown with the dash-dotted line. Notice that the dynamic length scale, has a composition dependence ($\varphi^{-0.26}$), intermediate to the purely intermolecular ($\varphi^{-0.6}$) and intramolecular (φ^0) length scales.

intermolecular pair correlation functions corresponding solely to the polymer. These results suggest that the pertinent length scale that best describes the slow segmental dynamics in miscible blends relates to both intra- and intermolecular contributions.

We thank Dr. M. Wagner (MPI-P) for NMR characterization. This research was supported by the Research Unit on Dynamics and Thermodynamics of the UoI (NSRF 2007-2013, Region of Epirus, call 18) and cofinanced by the European Union and Greek National Funds Research Funding Program: THALIS. Partially supported by the European Union's FP7-REGPOT-2009-1 project "Archimedes Center for Modeling, Analysis and Computation" (Grant No. 245749).

*Corresponding author.
gfloudas@cc.uoi.gr
†Corresponding author.
vagelis@tem.uoc.gr

[1] R. H. Colby, Polymer **30**, 1275 (1989).
[2] C. M. Roland and K. L. Ngai, Macromolecules **24**, 2261 (1991).
[3] Y. H. Chin, C. Zhang, P. Wang, P. T. Inglefield, A. A. Jones, R. P. Kambour, J. T. Bendler, and D. M. White, Macromolecules **25**, 3031 (1992).
[4] J. A. Pathak, R. H. Colby, G. Floudas, and R. Jérôme, Macromolecules **32**, 2553 (1999).
[5] Y. He, T. R. Lutz, and M. D. Ediger, J. Chem. Phys. **119**, 9956 (2003).
[6] E. Krygier *et al.*, Macromolecules **38**, 7721 (2005).
[7] K. L. Ngai and C. M. Roland, Rubber Chem. Technol. **77**, 579 (2004).
[8] A. Zetsche and E. W. Fischer, Acta Polym. **45**, 168 (1994).
[9] T. P. Lodge and T. C. B. McLeish, Macromolecules **33**, 5278 (2000).
[10] G.-C. Chung, J. A. Kornfield, and S. D. Smith, Macromolecules **27**, 964 (1994).
[11] S. K. Kumar, R. H. Colby, S. H. Anastasiadis, and G. Fytas, J. Chem. Phys. **105**, 3777 (1996).
[12] S. Kamath, R. H. Colby, S. K. Kumar, K. Karatasos, G. Floudas, G. Fytas, and J. E. L. Roovers, J. Chem. Phys. **111**, 6121 (1999).
[13] S. Shenogin, R. Kant, R. H. Colby, and S. K. Kumar, Macromolecules **40**, 5767 (2007).
[14] E. Leroy, A. Alegría, and J. Colmenero, Macromolecules **36**, 7280 (2003).
[15] D. Cangialosi, A. Alegría, and J. Colmenero, Macromolecules **39**, 7149 (2006).
[16] R. H. Colby and J. E. G. Lipson, Macromolecules **38**, 4919 (2005).
[17] W. Liu, D. Bedrov, S. Kumar, B. Veytsman, and R. Colby, Phys. Rev. Lett. **103**, 037801 (2009).
[18] G. Floudas, G. Fytas, T. Reisinger, and G. Wegner, J. Chem. Phys. **111**, 9129 (1999).
[19] G. A. Schwartz, J. Colmenero, and Á. Alegría, Macromolecules **40**, 3246 (2007).
[20] C. M. Roland and R. Casalini, Macromolecules **40**, 3631 (2007).
[21] A. Gitsas, G. Floudas, R. P. White, and J. E. G. Lipson, Macromolecules **42**, 5709 (2009).
[22] K. Mpoukouvalas and G. Floudas, Macromolecules **41**, 1552 (2008).
[23] G. Floudas, M. Paluch, A. Grzybowski, and K. L. Ngai, *Molecular Dynamics of Glass-Forming System: Effects of Pressure* (Springer, New York, 2011).
[24] G. Floudas, Prog. Polym. Sci. **29**, 1143 (2004).
[25] S. Salaniwai, R. Kant, R. H. Colby, and S. K. Kumar, Macromolecules **35**, 9211 (2002).
[26] D. Bedrov and G. D. Smith, Macromolecules **39**, 8526 (2006).
[27] M. Tyagi, A. Arbe, A. Alegría, J. Colmenero, and B. Frick, Macromolecules **40**, 4568 (2007).
[28] J. Maranas, Curr. Opin. Colloid Interface Sci. **12**, 29 (2007).
[29] V. Harmandaris, D. Angelopoulou, V. G. Mavrantzas, and D. N. Theodorou, J. Chem. Phys. **116**, 7656 (2002).
[30] V. Harmandaris, G. Floudas, and K. Kremer, Macromolecules **44**, 393 (2011).
[31] V. Harmandaris, D. Reith, N. F. A. van der Vegt, and K. Kremer, Macromol. Chem. Phys. **208**, 2109 (2007); Macromolecules **40**, 7026 (2007).
[32] J. E. G. Lipson and S. T. Milner, J. Polym. Sci. B **44**, 3528 (2006).
[33] See Supplemental Material at http://link.aps.org/supplemental/10.1103/PhysRevLett.110.165701 for the analysis of the DS and MD including the distribution of relaxation times for both processes.
[34] A. Deres, G. A. Floudas, K. Müllen, M. Van der Auweraer, F. De Schryver, J. Enderlein, H. Uji-i, and J. Hofkens, Macromolecules **44**, 9703 (2011).
[35] J. Colmenero and A. Arbe, Soft Matter **3**, 1474 (2007).